Journal of Sound and Vibration 329 (2010) 2884–2894

Contents lists available at ScienceDirect

Journal of Sound and Vibration

journal homepage: www.elsevier.com/locate/jsvi

Acoustic impedance at the interface between a plain and a perforated pipe

K.S. Peat *

Department of Aeronautical & Automotive Engineering, Loughborough University, Loughborough, Leicestershire LE11 3TU, UK

ARTICLE INFO

Article history:
Received 5 October 2009
Received in revised form
28 January 2010
Accepted 28 January 2010
Handling Editor: A.V. Metrikine

ABSTRACT

This paper considers the effective impedance that pertains as low frequency sound in a plain pipe radiates into a general perforated pipe of equal diameter. A previous theory that considered only the reactance is extended to also include resistance. Experimental measurements are made of the response of a Helmholtz resonator to an external sound field, where the neck of the Helmholtz resonator has both plain and perforated pipe sections. A complete theoretical model of this resonator allows for comparison between measured and predicted results of transfer functions from the external to internal sound fields of the resonator. The Nyquist plot of the admittance transfer function is extremely sensitive to the small resistance values, whereas the pressure transfer function gives more accurate results for resonant frequency and hence reactance than the usual method. In particular the results for resistance are so sensitive that it becomes possible to infer which of the current models for aperture resistance within the perforate is the most appropriate.

1. Introduction

Perforated pipes and plates feature commonly in the internal design of silencer systems. In absorption silencers they are used to physically separate the absorption material from the main air duct, whilst allowing acoustic waves to pass from the air duct into the absorbent relatively unimpeded. In flow duct silencers they are also used to help prevent the mean flow from expanding into the silencer volume, which would cause vortex generation and hence pressure loss, whilst again allowing acoustic waves to pass relatively unimpeded into the outer volume. In order to evaluate the overall acoustic effectiveness of such silencer systems it is essential to have an accurate knowledge of the acoustic impedance of the perforate or, more fundamentally, the impedance of an orifice in a plate.

Models for orifice and perforate impedance in the absence of any mean flow were proposed by Sivian [1], Ingard [2] and Melling [3]. In each case the model for resistance was to some extent empirical, since purely theoretical models did not agree with experimental measurements. While all three authors agree that the theoretical resistance is too low, they differ in their resultant empirical models. For perforates in the presence of grazing and/or bias mean flow, many empirical models have been proposed, see [4–6] for example. More recently theoretical models for perforate impedance in mean flow conditions have been developed, see [7–12] for example. It appears that the reactance of a perforate in grazing flow can be predicted accurately [11] but the resistance values do not show such good agreement with experiment. Thus in cases both with and without mean flow there is uncertainty as to the correct model for resistance.

* Tel.: +44 1509 227232; fax: +44 1509 227275.
E-mail address: K.S.Peat@lboro.ac.uk

0022-460X/$ - see front matter © 2010 Elsevier Ltd. All rights reserved.
doi:10.1016/j.jsv.2010.01.037

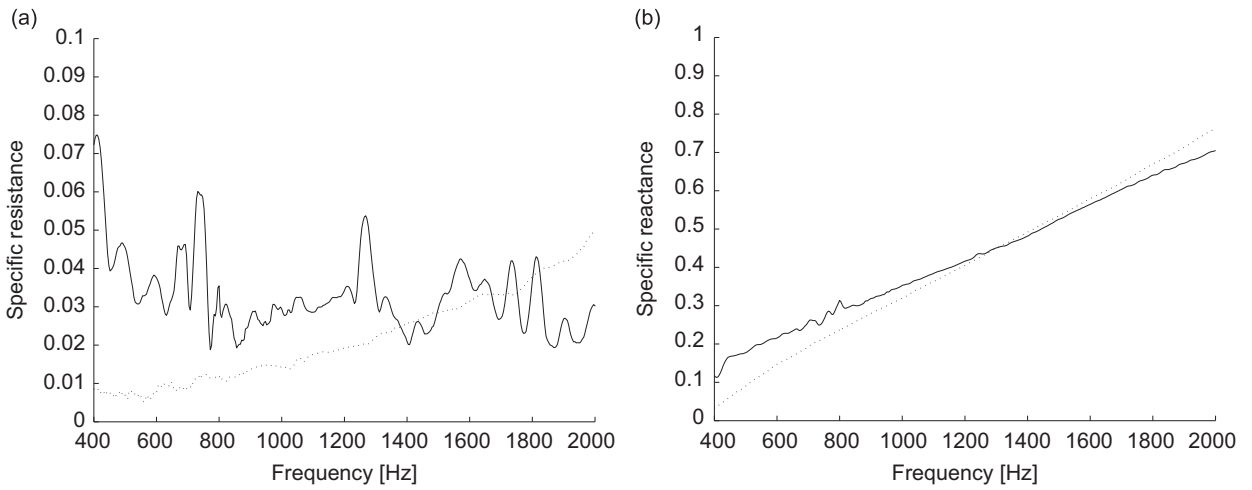

Fig. 1. Measured orifice impedance from different experimental setups [13]: —— bias flow setup, - - - - - grazing flow setup. (a) Resistance, (b) reactance.

The standard method of direct impedance measurement of a perforate in either grazing flow [6] or bias flow [12] results in a single complex measured value and, unless there is significant mean flow, the real part which constitutes the resistance is much smaller than the imaginary part, the reactance. Thus the resistance values are affected strongly by any measurement error and are thereby subject to greater uncertainty than the reactance values. In the absence of mean flow the impedance can be measured by either the grazing or bias flow experimental setup and a comparison between the two gives an indication of the measurement error. It is found [13] that the comparative reactance values are similar but that the resistance values are not, see Fig. 1 for an example. The absolute error of measurement for both the resistance and reactance values is the same, but the actual resistance values are so small that they cannot be discerned from the measurements. Thus what is required is a measurement method with large sensitivity to resistance by which the various models for resistance can be accurately assessed.

The reactance or end correction at the interface of a plain and a perforated pipe has been evaluated experimentally for perforates in mean flow [14] and both theoretically and experimentally for perforates without mean flow [15]. In both cases the experimental values were obtained by measuring the response of a Helmholtz resonator which had a neck in the form of a tube with both plain and perforated sections. For the with flow case, a second plain pipe neck was also required. The experimental end correction was obtained from a loss-free model of the Helmholtz resonator, once the resonant frequency had been obtained as the frequency of maximum response of the resonator to an external sound field. The theoretical end correction in the no-flow case resulted from an analytical model of the perforate, central to which was a model of the reactance of the orifices in the perforate.

This paper extends the previous work [15] to include resistance effects in the models of both the perforate and the Helmholtz resonator. Furthermore the experimental measurements are altered to record the pressure transfer function from the external to the internal sound field of the resonator. This gives a much more accurate measure of resonant frequency of the resonator and hence the experimental value of end correction. More importantly, standard techniques of modal analysis [16] show that the transfer function of the acoustic velocity response in the resonator to the external sound pressure gives rise to a Nyquist plot which ideally is a circle whose radius is essentially a function of resistance. This gives an extremely sensitive measure of the overall resistance of the resonator, from which the orifice resistance of the perforate can be inferred. It is shown that this approach is accurate enough to identify Ingard's model [2] for orifice resistance as the best of the current resistance models in the absence of mean flow. Attention is restricted to the linear regime of aperture impedance which, in the absence of mean flow, places a limit only on the amplitude of sound at the aperture [3]. The potential exists to extend this approach to consider mean flow effects using a two-pipe resonator setup [14].

2. Theory

In order to include resistive effects in the earlier theoretical model [15] of the system shown in Fig. 2 it is necessary to make developments in two separate areas. In the first instance, resistive effects must now be included in the lumped parameter model of the Helmholtz resonator. For this application it has been found necessary to modify the standard resistive lumped parameter model of a Helmholtz resonator [17] to also allow for nonrigid walls of the volume of the resonator. General techniques of modal analysis are then adapted to determine the input impedance to the perforate from an assumed measured transfer function. Secondly, the previous work on the model of a finite section of perforated pipe [15] is extended to give a fully theoretical estimate of the input impedance to the perforate.

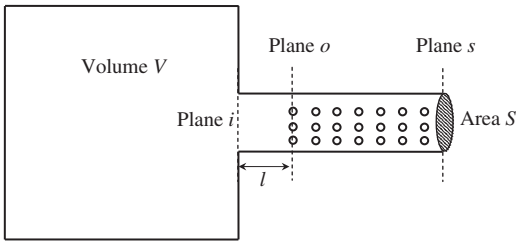

Fig. 2. Helmholtz resonator with plain and perforated sections of neck.

2.1. Resistive model of a Helmholtz resonator

Let the volume V of the resonator increase due to outward displacement x' of the air mass in the neck of the resonator and displacement w' of the walls of the resonator, such that the volume increase is

$$V' = Sx' + Aw', \tag{1}$$

where S and A are the cross-sectional area of the neck and the surface area of the volume respectively. Since the mass of air in the resonator is constant, then $\rho'/\rho = -V'V$ where ρ is the air density. If it is assumed that the acoustic fluctuations occur isentropically, then the acoustic pressure is

$$p' = \rho' c^2 = -\rho c^2 V'/V, \tag{2}$$

where c is the speed of sound. Let the volume have a surface impedance $\zeta_w = p'/(\rho c\dot{w}')$ such that, for harmonic sound of frequency ω, $\zeta_w = p'/(\mathrm{i}\omega w'\rho c)$, then it follows from Eqs. (1) and (2) that

$$x' = -\left(\frac{V}{c} + \frac{A}{\mathrm{i}\omega\zeta_w}\right)\frac{p'}{\rho c S}. \tag{3}$$

Next consider the mass of air m in the neck of the resonator. Let the acoustic pressures at the inlet plane i and outlet plane o of the neck be p_i' and p_o', respectively, and let the attenuation constant be α, such that the pressure drop per unit length [17] is $2\alpha\rho c\dot{x}'$, then

$$m\ddot{x}' = (p_i' - p_o' - 2\alpha\rho c l\dot{x}')S, \tag{4}$$

where the physical length of the neck is l. Let the impedance at inlet and outlet be ζ_i and ζ_o, respectively, where $p' - p_i' = \rho c\zeta_i\dot{x}'$, $p_o' - p_\infty' = \rho c\zeta_o\dot{x}'$ and p_∞' is the acoustic pressure external to the resonator, then

$$-\rho l\omega^2 x' = (p' - \mathrm{i}\omega\rho c\zeta_i x') - (p_\infty' + \mathrm{i}\omega\rho c\zeta_o x') - \mathrm{i}\omega 2\alpha\rho c l x'. \tag{5}$$

Substitution from Eq. (3) then gives

$$\frac{p_\infty'}{p'} = 1 - k^2\frac{lV}{S} + \frac{\mathrm{i}k}{S}\left[(\zeta_i + \zeta_o + 2\alpha l)V + \frac{lA}{\zeta_w}\right] + \frac{A}{\zeta_w S}(\zeta_i + \zeta_o + 2\alpha l), \tag{6}$$

where k is the wavenumber. Let $\zeta_i = r_i + \mathrm{i}kl_i$, $\zeta_o = r_o + \mathrm{i}kl_o$ where l_i, l_o are the effective end corrections at inlet and outlet, respectively, then

$$\frac{p'}{p_\infty'} = \frac{1}{\upsilon + \mathrm{i}kv} = \frac{\upsilon - \mathrm{i}kv}{\upsilon^2 + k^2 v^2}, \tag{7}$$

where

$$\upsilon = 1 + \frac{A}{\zeta_w S}(r_i + r_o + 2\alpha l) - k^2\frac{(l + l_i + l_o)V}{S} \tag{8}$$

and

$$v = \frac{1}{S}\left[(r_i + r_o + 2\alpha l)V + \frac{(l + l_i + l_o)A}{\zeta_w}\right]. \tag{9}$$

One can now apply the classic modal analysis techniques of a single degree of freedom system [16]. Firstly from Eqs. (7) and (8), $\mathrm{Re}\{p'/p_\infty\} = 0$ when

$$k^2 = \left[1 + \frac{A}{\zeta_w S}(r_i + r_o + 2\alpha l)\right]\frac{S}{(l + l_i + l_o)V} \tag{10}$$

and secondly

$$\left[\mathrm{Re}\left(\mathrm{i}k\frac{p'}{p_\infty'}\right) - \frac{1}{2v}\right]^2 + \left[\mathrm{Im}\left(\mathrm{i}k\frac{p'}{p_\infty'}\right)\right]^2 = \left(\frac{1}{2v}\right)^2. \tag{11}$$

If the pressure transfer function p'/p'_∞ is measured experimentally as a function of frequency, then the frequency and hence wavenumber in Eq. (10) at which the real part of the transfer function becomes zero can be simply and precisely determined. Furthermore, Eq. (11) implies that a Nyquist plot of the real versus imaginary parts of the measured values of $(ikp')/p'_\infty$, hereafter referred to as the admittance transfer function, will result in a circle of centre $(1/2v, 0)$, radius $1/2v$, from which v can be measured. This procedure assumes that v is constant, whereas in reality it is not, since r_i, r_o and α are all functions of wavenumber. This complication is ignored for the moment but will be reviewed later. Now, if one assumes that all of the variables in the right-hand sides of Eqs. (9) and (10) are known except for r_o and l_o, then the measured values of v and k at $\mathrm{Re}\{p'/p'_\infty\} = 0$ result in two coupled equations from which to determine r_o and l_o. These values, that derive from experimental measurements, can be compared with theoretical values as determined below.

It should be noted that the coupling between Eqs. (9) and (10) only occurs through the impedance of the resonator walls, ξ_w. If the resonator volume were perfectly rigid, $\xi_w \to \infty$, there would be no coupling at all. Since in most practical applications, including the resonator used in the experiments in Section 3, the walls of a resonator volume are almost rigid, then the coupling is very small and Eqs. (9) and (10) are to first-order separate equations for r_o and l_o, respectively.

2.2. Theoretical input impedance of a finite perforated tube

Consider, as in [15], low frequency plane-wave acoustic propagation in a uniform plain pipe of radius a ($S=\pi a^2$) that connects to a perforated pipe of similar radius at plane o, see Fig. 3a. The perforated pipe is assumed to consist of n identical sections, where each section has a single ring of N circular holes of radius b followed by a plain pipe section of length L and radius a, see Fig. 3b. For a general section j, the acoustic pressure p and particle velocity u of the plane wave before (subscript 1) and after (subscript 2) the ring of holes are related by

$$\begin{bmatrix} p_1 \\ \rho c u_1 \end{bmatrix} = \begin{bmatrix} 1 & 0 \\ \dfrac{N}{\zeta_h}\left(\dfrac{b}{a}\right)^2 & 1 \end{bmatrix} \begin{bmatrix} p_2 \\ \rho c u_2 \end{bmatrix}, \tag{12}$$

where $\zeta_h = p_1/\rho c u_h$ is the specific impedance of a single hole. Similarly the acoustic pressure and velocity at inlet (subscript 2) and outlet (subscript 3) of a plain pipe of length L can be related by a transfer matrix, namely [18]

$$\begin{bmatrix} p_2 \\ \rho c u_2 \end{bmatrix} = \begin{bmatrix} \cos(k'L) & \mathrm{i}\sin(k'L) \\ \mathrm{i}\sin(k'L) & \cos(k'L) \end{bmatrix} \begin{bmatrix} p_3 \\ \rho c u_3 \end{bmatrix}, \tag{13}$$

where the use of $k' = k(1 - \mathrm{i}\alpha/k)$ accounts for viscous losses along the pipe. Let the holes have thickness t, the wall thickness of the perforated pipe. Typically t, $b < a$ and therefore, since this is a low frequency plane-wave analysis, kt, $kb \ll 1$. The specific impedance of a single aperture is then [3]

$$\zeta_h = 2\alpha(t + \eta b) + (kb)^2 + \mathrm{i}k\left(t + \frac{16b}{3\pi\psi(\xi)}\right), \tag{14}$$

where [19] the Fok function $\psi(\xi)$, with $\xi = b/B$, accounts for the interaction effects between holes and B is the radius of the zone area per hole. The correct value of η is a matter of debate and is discussed at length in Section 4. Multiplication of the transfer matrices of Eqs. (12) and (13) gives the transfer matrix of a single section of the perforated pipe, namely one ring of N holes and one intermediate pipe of length L. Thus the transfer matrix from inlet plane o to outlet plane s of a perforated

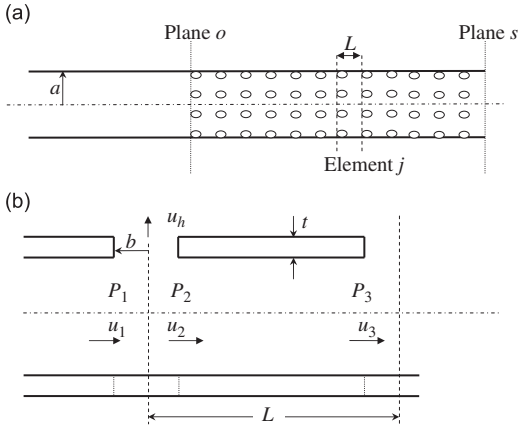

Fig. 3. (a) Pipe termination and perforate. (b) General jth element of the perforate.

tube, composed of n such sections, is given by

$$\begin{bmatrix} p_o \\ \rho c u_o \end{bmatrix} \approx \begin{bmatrix} \cos(k'L) & \mathrm{i}\sin(k'L) \\ \phi\cos(k'L)+\mathrm{i}\sin(k'L) & \cos(k'L)+\mathrm{i}\,\phi\sin(k'L) \end{bmatrix}^n \begin{bmatrix} p_s \\ \rho c u_s \end{bmatrix} = \begin{bmatrix} A & B \\ C & D \end{bmatrix} \begin{bmatrix} p_s \\ \rho c u_s \end{bmatrix}, \tag{15}$$

where $\phi = (N/\zeta_h)(b/a)^2$. Hence

$$\zeta_o \equiv \frac{p_o}{\rho c u_o} = r_o + \mathrm{i}\,k l_o = \left(\frac{A\zeta_s + B}{C\zeta_s + D}\right), \tag{16}$$

where ζ_s is the classic radiation impedance [20] from a pipe of radius a into free space.

3. Experimental measurements

The experiment was conducted inside an anechoic chamber with a setup as shown in Fig. 4. A loudspeaker was placed a large and equal distance from an external microphone and the pipe-perforate interface on the neck of a Helmholtz resonator. The sound pressure level at this microphone and hence the perforate was maintained at less than 90 dB such that, in conformity with the theoretical approach above, the aperture impedance would be restricted to the linear regime [3]. A second microphone measured the internal pressure within the resonator volume. A swept-sine signal was input to the loudspeaker and the pressure transfer function between the two microphones was measured directly by a sound analyser. The hardware, in terms of the resonator volume and the variety of necks used, is shown in Fig. 5 and is identical to that used in earlier studies [14,15]. The resonator volume was cylindrical with internal length 127 mm and radius 73.5 mm. The necks all consisted of a plain pipe section of length 35 mm and radius 21 mm and one neck consisted of this plain pipe section only. The perforated sections were all of the same length and had holes of the same size and pattern, but differed in porosity between 4.4% and 16.1%. Experimental measurements of the pressure transfer function relevant for each neck were repeated three times whilst the setup was unchanged. Repeatability under these conditions was excellent, with no discernible difference upon ultimate values for end correction and resistance. The experiments for all perforates were also repeated on three separate occasions, any given neck having been removed and replaced between each of these tests. This did give rise to a noticeable variation between results and the three test cases referred to below refer to these three separate test occasions and setups.

In the first instance, for each test sequence the plain pipe neck of length 35 mm and radius 21 mm, shown in Fig. 5, was used. In the case of a plain pipe, the impedance at the outer end of the neck is that for radiation from an open end of a pipe into free space [20], namely $\zeta_o = r_o + \mathrm{i}kl_o = (ka)^2/4 + \mathrm{i}k(0.61a)$, where a is the pipe radius. At the inner end, the impedance is that for radiation from an open end of a pipe into half-space [21], modified by the Karal correction factor [22] $H(\beta)$ to account for the presence of the resonator volume, namely $\zeta_i = r_i + \mathrm{i}kl_i = (ka)^2/2 + \mathrm{i}k[(8/3\pi)aH(\beta)]$, where β is the ratio of radii. The attenuation constant α is also known [17], hence the only unknown in Eqs. (7)–(9) is the surface impedance of the resonator volume $\zeta_w = (1+W)/(1-W)$, where W is the corresponding reflection coefficient. If it is assumed that the resonator volume has perfectly rigid walls, such that $W=1$, then the comparison between the theoretical and experimental Nyquist plots of the admittance transfer function, Eq. (11), is extremely poor, as shown in Fig. 6. It is for this reason that the wall impedance was introduced into the theory of Section 2.1. The required value for the reflection coefficient is obtained so as to give the best fit of theoretical as compared to experimental Nyquist plots, as shown in Fig. 7. The theoretical Nyquist plot is extremely sensitive to the reflection coefficient W. The value used for Fig. 7 was 0.9942 and a change in the third significant figure causes about a 10% change in radius. It is not to be inferred that this is the precise value of the average reflection coefficient at the resonator walls. Rather this value serves to give very close agreement between experimental and theoretical values and helps cover any deficiencies within the resistance models of the plain pipe neck and its terminations. The only difference to the model between a plain pipe neck and a partially perforated neck is in the value of ζ_o. In the case of the plain pipe, the theoretical value of ζ_o is known to a high level of accuracy and also has minimal contribution towards the overall resistance value. Thus by selection of the value of W to give near perfect agreement for the case of a plain pipe neck, it is assured that future differences between experimental and theoretical values are due entirely to the perforates. The two further test sequences required W values of 0.9935 and 0.9953 to give perfect agreement for the

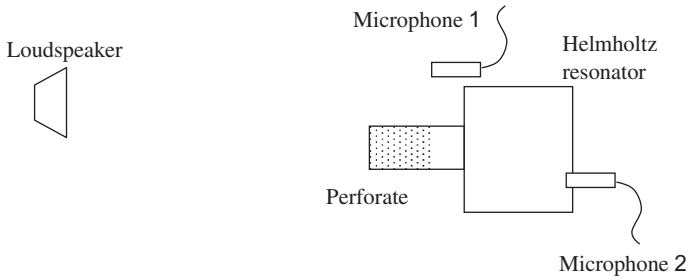

Fig. 4. Experimental setup.

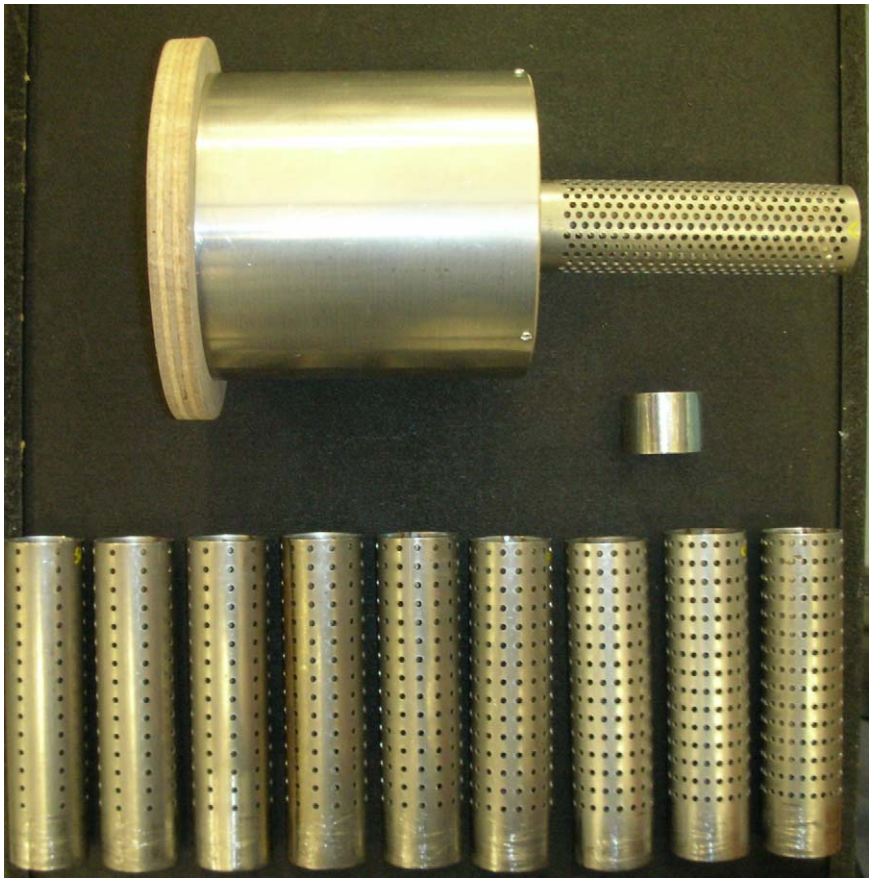

Fig. 5. Helmholtz resonator and the plain/perforated necks used in the experiments.

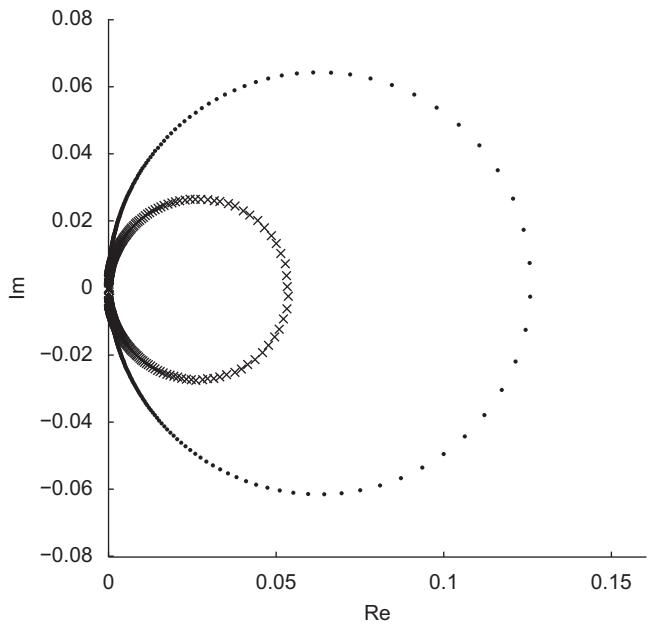

Fig. 6. Nyquist plot of the admittance transfer function for a plain pipe neck. x experimental values; • theoretical values with $W=1$.

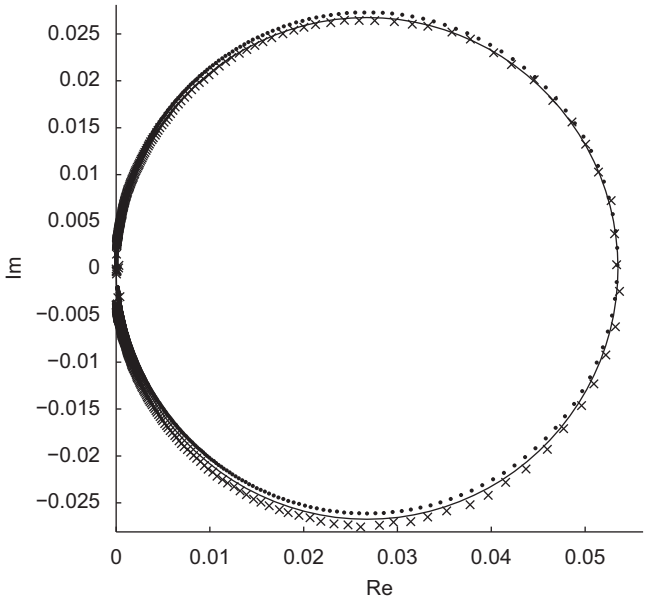

Fig. 7. Nyquist plot of the admittance transfer function for a plain pipe neck. x experiment; • theory with W=0.9942; —— perfect circle.

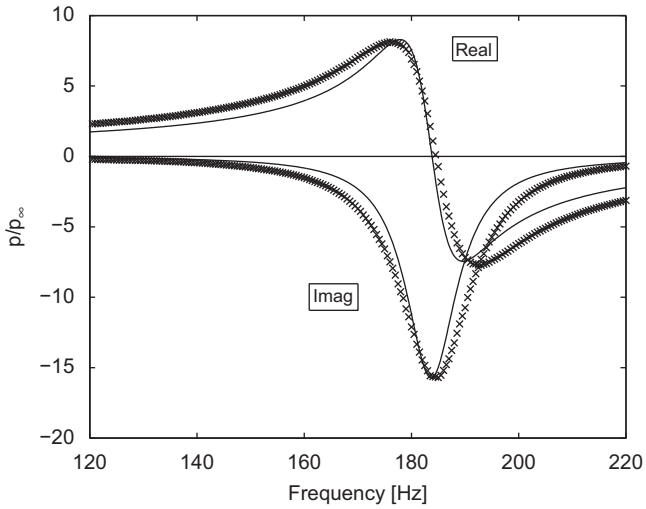

Fig. 8. Pressure transfer function for a plain pipe neck. × experiment; —— theory.

plain pipe neck. The reason for the variation is most likely due to slight changes in the efficiency of the sealing of the resonator when assembled on different occasions.

As noted in Section 2.1, v from Eq. (9) is a function of wavenumber and hence the Nyquist plots of the admittance transfer function for a Helmholtz resonator will not be perfectly circular. A perfect circle centred on the real axis is shown in Fig. 7, by comparison to which it can indeed be seen that neither the experimental or theoretical Nyquist plots are exactly circular. However, the plots are close enough to being circular such that an estimated radius of the 'circle' can be meaningfully deduced to give an effective constant value of v. In particular, the symbols in Fig. 7 that pertain to the resonant condition are those furthest from the origin of coordinates and thus the required 'radius of circle' v is best evaluated with reference to this data.

Once the value of W, and hence ζ_w, has been inferred from the Nyquist plots, then Eq. (10) can be used to evaluate the theoretical resonant frequency to compare with that measured. Fig. 8 shows both real and imaginary parts of the pressure transfer function against frequency, although it is only the frequency at which the real part becomes zero that is actually used. It is apparent from the figure how precisely the experimental value of resonant frequency can be determined by this technique, much more precisely than by trying to estimate the centre point of a resonant peak as was done in earlier works [14,15]. As shown in Fig. 8, the real parts of both theoretical and experimental plots do not cross through zero at exactly the

same frequency. However over the three separate series of test results the average resonant frequency from the test results is virtually identical to the theoretical value. The reason for the variation between experiments is most likely due to very slight differences in the insertion length of the resonator neck into the end plate of the resonator volume, which ideally would result in a perfectly flush fit at the inner surface of the end plate.

4. Discussion of results for perforates

The wavenumber at which the real part of the pressure transfer function was zero and the effective radius of the Nyquist plot of the admittance transfer function were each deduced from the measured data and used in Eqs. (10) and (11) to give a pair of simultaneous equations for the measured values of r_o and l_o, the effective resistance and end correction at the junction between the plain and perforated pipe sections. These are then compared with the respective theoretical values from Eq. (16). These theoretical values depend upon the theoretical impedance of an orifice, Eq. (14), and as noted earlier there is some debate about the correct expression for resistance, specifically with respect to the value of η.

The experimental and theoretical results for end correction are shown in Fig. 9 and are seen to be in good agreement. The value $\eta=2$ was used in the theoretical calculations but, as noted earlier, the coupling between Eqs. (10) and (11) is very weak and the results do not visibly alter whatever rational value of η is used in of the resistance model. It can also be seen in Fig. 9 that the experimental values have much less scatter than those measured earlier [15] when the resonant frequency was estimated from the frequency of peak response.

The acoustic resistance of a pipe is usually evaluated in theory as the sum of the visco-thermal resistance along the wall of the pipe together with the radiation resistance at each end. If an orifice is regarded as a short pipe with two flanged ends, at each of which the radiation resistance is that from a flanged pipe [21], then the overall orifice resistance corresponds to $\eta=0$ in Eq. (14). This was found [1–3] to result in an under-prediction of the overall resistance of an orifice. Thus Sivian [1] proposed use of the wall resistance in a tube whose length was the sum of the physical thickness of the aperture t and the effective end corrections of the aperture reactance. To be precise the viscosity Sivian used for the end correction element was the thermal viscosity μ' only, giving $\eta=16\mu'/3\pi\mu$ but, even with this proviso, there appears to be scant physical justification for this approach. In contrast Ingard [2] looked for an extra contribution to the resistance that is missing from the first approach. Thus he took account of the viscous effects on the flanged walls surrounding the aperture and deduced that $\eta=1$. However this did not give good agreement with experimental results and he found $\eta=2$ to be better. The required increase was explained because the influence of the acoustic flow around the sharp corners of an orifice may be expected to contribute significantly to the total viscous resistance but was not accounted for in the analysis. Melling [3] surmised that, in order to take account of interference effects when these expressions for a single aperture are used for the resistance of perforates, one should divide the extra terms arising from the end effects by the Fok function, in the same manner as for the reactive end correction. This gives in Ingard's case, say, a value of $\eta=2/\psi(\xi)$. Whilst it cannot be disputed that there will be some interference effect upon the resistance, it should be noted that the derivation of the Fok function is from a potential flow analysis explicitly for the reactance only and, from a physical viewpoint, one would not expect an identical interference effect for resistance.

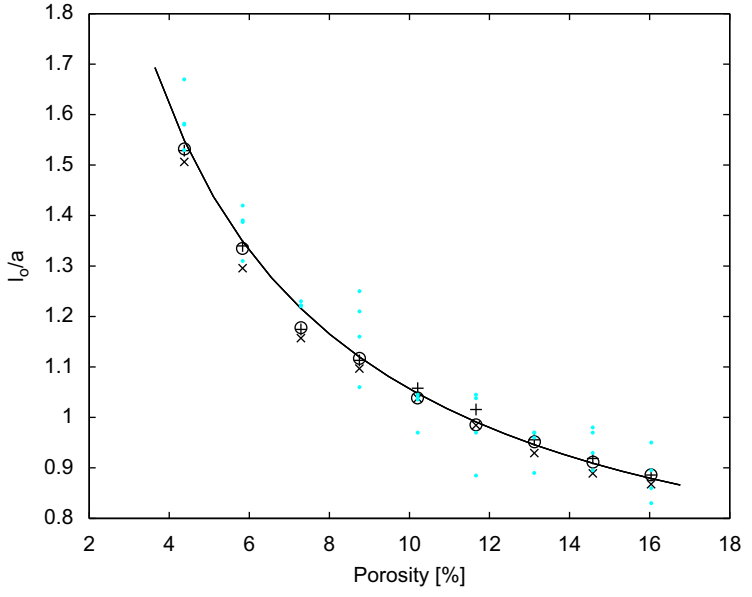

Fig. 9. End correction at a pipe-perforate interface as a function of perforate porosity. Experiment: ×, +, ○; earlier experiment [15]; theory: ——.

The theoretical values of the pipe-perforate resistance $r_o/(ka)^2$ as a function of perforate porosity that result from these various forms of η within the orifice resistance are shown in Fig. 10 in comparison to experimental values. It is seen from Fig. 10 that Ingard's [2] equation, $\eta=2$, gives the most accurate comparison of theoretical to experimental results, in terms of both magnitude and trend. In particular, use of the Fok function to account for resistive interaction between holes does not appear to be justified. This could be interpreted as a justification of Ingard's assertion that the extra resistance term is largely controlled by effects at and close to the sharp corners of an orifice. Furthermore it may be noted that the radiation resistance makes minimal contribution to the overall resistance and thus potential effects of interference upon the radiation resistance are inconsequential.

Nyquist plots of the admittance transfer function for the two extremes of perforate porosity tested, namely 4.4% and 16.1%, are shown in Figs. 11 and 12. Experimental results are compared against theoretical results for two cases, namely $\eta=2$ and $\eta=16\mu'/3\pi\mu\psi(\xi)$. The latter would appear, from Fig. 10, to be the only serious contender with $\eta=2$ for the most accurate of resistance models currently proposed. It is clear how very sensitive the Nyquist plots are to changes in

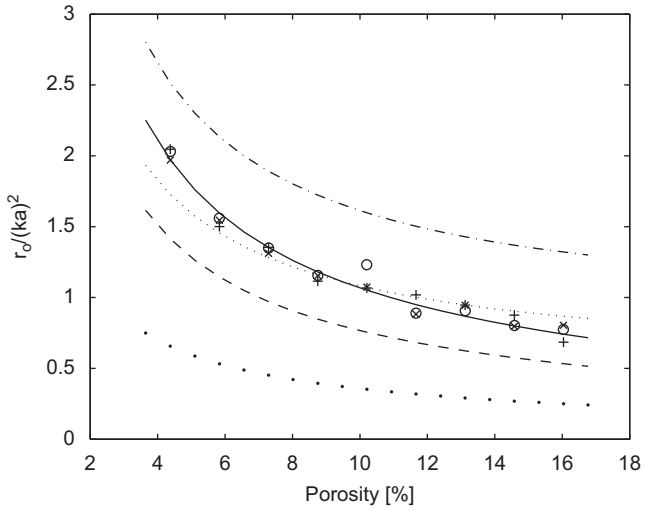

Fig. 10. Resistance at a pipe-perforate interface as a function of perforate porosity. Experiment: ×, +, ○; theory: • $\eta=0$, ——— $\eta=2$, — - — $\eta=2/\psi(\xi)$, —— —— $\eta=16\mu'/3\pi\mu$, - - - - - $\eta=16\mu'/3\pi\mu\psi(\xi)$.

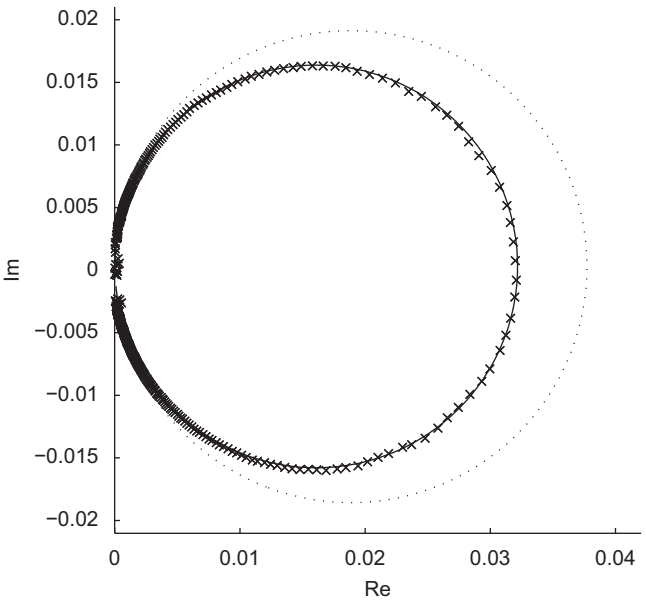

Fig. 11. Nyquist plot of the admittance transfer function for a perforate of 4.4% porosity. Experiment: ×; theory: ——— $\eta=2$, - - - - - $\eta=16\mu'/3\pi\mu\psi(\xi)$.

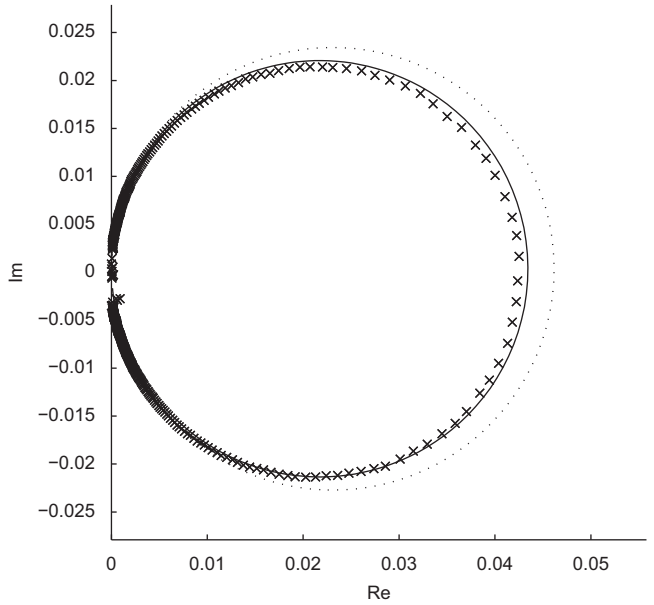

Fig. 12. Nyquist plot of the admittance transfer function for a perforate of 16.1% porosity. Experiment: $\times$; theory: —— $\eta=2$, - - - - - $\eta=16\mu'/3\pi\mu\psi(\xi)$.

measured or predicted hole resistance and the case for the adoption of $\eta=2$ is even more compelling from these figures than from Fig. 10.

5. Conclusions

Measurement of the pressure and admittance transfer functions for the response of a Helmholtz resonator to an external pressure field enable accurate determination of both the resistance and end correction at the outlet of the plain pipe section of a resonator neck. If the neck consists of plain and perforated pipe sections, this leads in turn to accurate measurement of the resistance and end correction at the interface between a plain and a perforated pipe. These values have been compared to the theoretical values that result from an acoustic model of the perforate. Various existing models of the impedance of an orifice have been used within the perforate model and comparison with experimental results indicates the model of Ingard [2] to be the most accurate.

Acknowledgment

The author is grateful to Dr S.-H. Lee and Prof. J.-G. Ih for making available to me their experimental data with permission to use it in Fig. 1.

References

[1] L.J. Sivian, Acoustic impedance of small orifices, *Journal of the Acoustical Society of America* 7 (1935) 94–101.
[2] U. Ingard, On the theory and design of acoustic resonators, *Journal of the Acoustical Society of America* 25 (1953) 1037–1061.
[3] T.H. Melling, The acoustic impedance of perforates at medium and high sound pressure levels, *Journal of Sound and Vibration* 29 (1973) 1–65.
[4] A.B. Bauer, Impedance theory and measurement on porous acoustic liners, *Journal of Aircraft* 14 (1977) 720–728.
[5] K.N. Rao, M.L. Munjal, Experimental evaluation of impedance of perforates with grazing flow, *Journal of Sound and Vibration* 108 (1986) 283–295.
[6] S.-H. Lee, J.-G. Ih, Empirical model of the acoustic impedance of a circular orifice in grazing mean flow, *Journal of the Acoustical Society of America* 114 (2003) 98–113.
[7] M.S. Howe, On the theory of unsteady high Reynolds flow through a circular aperture, *Proceedings of the Royal Society A* 366 (1979) 205–223.
[8] M.S. Howe, M.I. Scott, S.R. Sipcic, The influence of tangential mean flow on the Rayleigh conductivity of an aperture, *Proceedings of the Royal Society A* 452 (1996) 2302–2317.
[9] X.D. Jing, X.F. Sun, J. Wu, K. Meng, Effect of grazing flow on the acoustic impedance of an orifice, *A.I.A.A. Journal* 39 (2001) 1478–1484.
[10] X.D. Jing, X.F. Sun, Effect of plate thickness on impedance of perforated plates with bias flow (2000), *A.I.A.A. Journal* 38 (2000) 1573–1578.
[11] K.S. Peat, R. Sugimoto, J.L. Horner, The effects of thickness on the impedance of a rectangular aperture in the presence of a grazing flow, *Journal of Sound and Vibration* 292 (2006) 610–625.
[12] S.-H. Lee, J.-G. Ih, K.S. Peat, A model of acoustic impedance of perforated plates with bias flow considering the interaction effects, *Journal of Sound and Vibration* 303 (2007) 741–752.

[13] S.-H. Lee, A Study on the Acoustic Characterization of Perforated Elements in the Presence of Flow, PhD Thesis, Korea Advanced Institute of Science and Technology, 2006.
[14] K.S. Peat, End corrections due to perforated pipes, *Bulletin of the Institute of Acoustics* 33 (1) (2008) 22–25.
[15] K.S. Peat, End correction at the interface between a plain, a perforated pipe, *Journal of Sound and Vibration* 319 (2009) 1097–1106.
[16] D.J. Ewins, *Modal Testing: Theory and Practice*, John Wiley, New York, 1984.
[17] L.E. Kinsler, A.R. Frey, A.B. Coppens, J.V. Sanders, *Fundamentals of Acoustics*, 4th ed, John Wiley, New York, 2000.
[18] M.L. Munjal, *Acoustics of ducts and mufflers*, John Wiley, New York, 1987.
[19] S.N. Rschevkin, *A course of lectures on the theory of sound*, Pergamon Press, London, 1963.
[20] M. Levine, J. Schwinger, On the radiation of sound from an unflanged circular pipe, *Physical Review* 73 (1948) 383–406.
[21] Lord Rayleigh, *Theory of Sound* (two volumes), Dover Publications, New York, 1877, re-issued 1945.
[22] F.C. Karal, The analagous acoustical impedance for discontinuities and constrictions of circular cross section, *Journal of the Acoustical Society of America* 25 (1953) 327–334.